Intracellular Pattern Formation: A Spatial Stochastic Model of Bacterial division site selection proteins MinCDE

Joshua L. Adelman*, Steven S. Andrews†

*Biophysics Graduate Group, University of California, Berkeley, CA 94720; †Physical Biosciences Division, Lawrence Berkeley National Laboratory, Berkeley, CA 94720
E-mail: jadelman@ocf.berkeley.edu

Bacterial division site selection is regulated by members of the Min-protein system. In *Escherichia coli* MinC, MinD, and MinE oscillate from pole to pole of the cell with a periodicity of approximately 40 sec. The region of lowest concentration of the Z-Ring inhibitor, MinC occurs at the center of the cell, confining the placement of FtsZ and thus defining the cell division site. In addition to its oscillatory behavior, it has been shown that MinD forms filamentous structures *in vivo* and *in vitro*. The mechanism for this phenomena remains unclear. We show that filament formation can be explained by a model based on *in vitro*-observed interactions.

The spatial organization of proteins within the cell plays a central role in the regulation of molecular processes. Until recently however, prokaryotic cells were thought to be relatively uniform at the subcellular level, distinguishing them from eukaryotic species. Recent advances in fluorescent imaging and other molecular techniques reveal a different story. Bacteria, like their eukaryotic brethren, segregate their internal host of proteins into different regions. Beyond just targeting particular proteins to specific regions of the cell, some proteins organize into discrete structures. It has been shown that *Bacillus subtilis* contains actin homologs MreB and Mbl, which form spirals along the long axis of the cell, and FtsZ which forms a tubulin-like ring during cytokinesis [1, 2]. While these examples constitute bacterial cytoskeletal elements, Shih *et al.* demonstrated that non-cytoskeletal components MinD and MinE also form ordered structures within the cell [3]. Previous to their study of this system, these proteins were thought to diffuse from one pole of the cell to the other in an oscillatory manner, binding to the inner-cellular membrane in an unordered fashion.

In *Escherichia coli*, the Min family of proteins constitutes one of the primary regulatory mechanisms responsible for placement of the cell division site through its modulation of FtsZ. *In vivo* FtsZ assembles into a ring-like structure (the Z ring), onto which a cascade of proteins attach to direct invagination of the cell membrane during division. MinC acts as an inhibitor of FtsZ polymerization, via its association with MinD on the inner-membrane. MinE in turn negatively regulates MinD by removing it and MinC from the membrane [4]. This scheme results in the accumulation of MinD and MinC in a membrane-associated polar zone at one end of the cell, followed by their removal and redistribution to the opposite end of the cell. Many oscillations of this nature occur during the division cycle, yielding a time-averaged lowest concentration of the MinC inhibitor at the midcell [3]. A mutation in MinC, resulting in the MinC^- phenotype, produces nucleoid-free non-viable minicells. A defect in MinE (Sep^-), causes a uniform distribution of MinD, and by association, MinC over the entire membrane. As this blocks all potential Z-ring assembly sites, cells form long nonseptate filaments[5] .

Several models have been posited to describe the mechanism of Min protein oscillations. Each model reproduces oscillations, but many contain specious biological assumptions that deviate from experimental observations *in vivo*. Meinhardt and de Boer's model [5] requires the synthesis and degradation of MinD and MinE, although

experimentally, blocking new protein synthesis did not effect Min oscillations [6]. The model of Howard, Rutenberg, and de Vet (HRdV) [7] requires that MinE is recruited to the membrane by cytoplasmic MinD, although evidence supports interaction with membrane-bound MinD instead [8]. Additionally, oscillation periodicity has the opposite dependency on MinD concentration, and MinD forms a medial band, again in direct conflict with experimental observations [6]. The model of Kruse [9] requires unrealistically rapid diffusion of membrane-bound MinD, while a recent stochastic version of the HRdV model [10], suffers from the assumptions that MinD is not recruited to membrane by MinD, and that MinE is driven onto the membrane by cytoplasmic MinD.

The model of Huang, *et al.* [6], currently provides the most realistic model of Min oscillations, and is able to reproduce several mutant phenotypes within its framework. However it is insufficient for several key reasons, as are most of the models previously cited. Most do not account for low copy-number fluctuations, none account for full three dimensional protein distributions including surface patchiness, none account for the fact that MinD recruitment must be a highly local process, and none reproduce observed helix formation.

A Spatial Stochastic Model Based on Reported *in Vitro* Molecular Interactions

The interactions governing Min protein dynamics are specified by the cycle described in the model of Huang, *et al* [6]. MinD:ATP is competent to associate with the cytoplasmic face of the cell membrane in a self-enhancing manner, such that it binds with greater affinity adjacent to other MinD:ATP. MinE binds to MinD:ATP on the membrane, activating its ATPase activity, causing both MinD and MinE to release from the membrane into the cytoplasm. MinD in its ADP bound state (MinD:ADP), must, through nucleotide exchange, convert back into MinD:ATP before binding to the membrane again (fig. 1). MinC is not explicitly accounted for as it is known to follow the pattern of MinD binding.

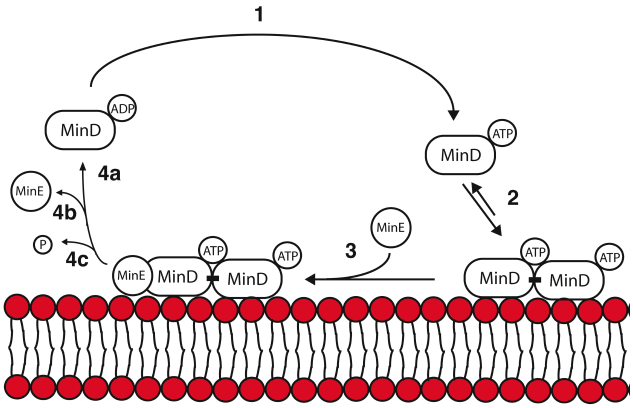

Figure 1: **Minimal Min D,E cycle:** **(1)** MinD:ADP is converted into MinD:ATP by nucleotide exchange. **(2)** MinD:ATP in the cytoplasm associates with the membrane cooperatively with other MinD:ATP already attached on the inner-membrane. This process is assumed to be reversible, whereas MinD:ATP binds transitively and can potentially rebind rapidly at a different membrane site. **(3)** MinE in the cytoplasm binds to the membrane-associated MinD:ATP. **(4)** MinE activates MinD's ATPase activity, disassociating (a) MinD:ADP, (b) MinE, (c) phosphate from the growing MinD:ATP complex and releasing each component into the cytoplasm.

Huang, *et al*, modeled this cycle as a set of coupled nonlinear partial differential equations, discretized on a 2D lattice in cylindrical coordinates. This framework must be recast in an attempt to capture the new levels of detail elucidated by recent experiments.

Dynamics and Numerical Methods

The model presented in this paper uses Smoluchowski dynamics, in which molecules are treated as individual particles that move through the system via diffusion. Inertial contributions are ignored, as are explicit interactions with the solvent. This level of representation lacks the detail and accuracy of atomic level, molecular dynamics calculations, but can elucidate the stochastic behavior of low copy number species, unavailable with differential equation based reaction-diffusion models. The theoretical foundations of Smoluchowski dynamics are described in ref. [11], however only the most basic framework is summarized here. In modeling the internal protein dynamics of the cell, it is assumed that there are no external forces acting

on the individual particles, other than the thermal fluctuations that give rise to diffusion. This leads to Fick's laws, that for a generic species A, are

$$\mathbf{J}_A(\mathbf{r},t) = -D_A \nabla \rho_A(\mathbf{r},t) \tag{1}$$

$$\dot{\rho}_A(\mathbf{r},t) = D_A \nabla^2 \rho_A(\mathbf{r},t) \tag{2}$$

$\mathbf{J}_A(\mathbf{r},t)$ is the flux of molecules of species A at a position $\mathbf{r}$ at time t, $\rho_A(\mathbf{r},t)$ is the number concentration of A, and D_A is the diffusion coefficient for species A. In order to implement this description of the physical processes numerically we must reinterpret eqns. 1 and 2. In treating each molecule as an individual particle, Fick's second law (eqn.2), must be written in terms of a spatial probability density,

$$\dot{p}_A(\mathbf{r},t) = D_A \nabla^2 p_A(\mathbf{r},t) \tag{3}$$

$p_A(\mathbf{r},t)d\mathbf{r}$ is the probability of finding a particular molecule of species A within the volume $d\mathbf{r}$ about the coordinate $\mathbf{r}$ at time t. During a time Δt, a molecule starts from a well-defined position and diffuses a distance, whose probability density is described by a Gaussian profile in each Cartesian coordinate,

$$p_A(\mathbf{r}+\Delta\mathbf{r}, t+\Delta t) = G(\Delta x)G(\Delta y)G(\Delta z) \tag{4}$$

$$G(\Delta x) = \frac{1}{s\sqrt{2\pi}} exp\left(-\frac{\Delta x^2}{2s^2}\right) \tag{5}$$

$$s = \sqrt{2D_A \Delta t} \tag{6}$$

$G(\Delta x)$ is a normalized Gaussian distribution with mean 0 and a standard deviation of s, where s is the root mean square step length of the molecular species. The Brownian motion or diffusion of each molecule is then simulated by selecting a normally distributed random displacement during each time step. A look-up table is generated to increase the speed of this algorithm, where the i^{th} entry of the table is

$$X_i = \sqrt{2} erf^{-1}\left(\frac{2i+1}{n} - 1\right) \tag{7}$$

In this simulation, the look-up table contains 2^{12} random numbers. To obtain the desired normally distributed random displacement, X_i is multiplied by s.

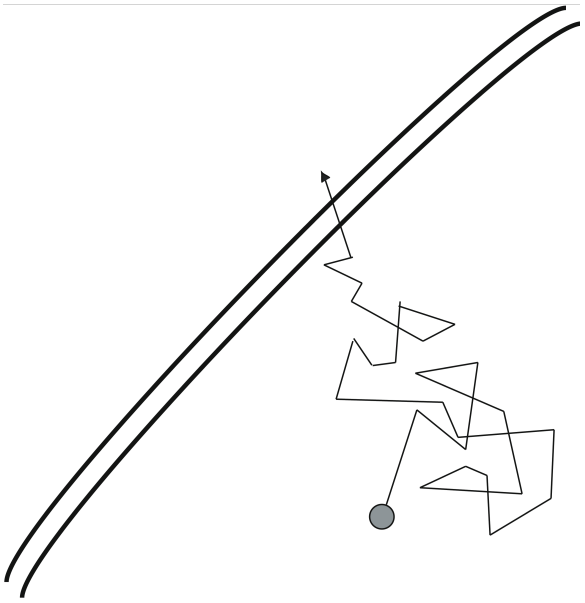

Figure 2: **Simulated Representation of Brownian Motion:** Schematic representation of a single molecule's (gray sphere) trajectory inside the cytoplasm of the cell. The last step in the trajectory takes it beyond the boundary of the system.

Surface Dynamics and Membrane Interactions

Geometrically, the shape of *E. coli* is well-approximated as a cylinder, although at this time it is unclear what effect the hemispherical 'caps' at either end of a real cell might have on internal dynamics. The cellular membrane is approximated by a hexagonal lattice with periodic boundary conditions on a single set of parallel edges. Wrapping the lattice in this fashion encloses the continuous space representing the cytoplasm. With the exception of the conversion of MinD:ADP to MinD:ATP, all chemical reactions in this system occur either with the membrane or on the membrane surface. As such, the hexagonal lattice is considered an absorbing boundary; the end caps of the cylinder are treated as impermeable or reflecting boundaries that are inert in terms of interactions with the molecules diffusing in the cytoplasm.

The absorbing boundary is treated by temporarily considering it to be permeable to the passage of molecules that start in the cytoplasm and diffuse out

of the volume of the cell. It is assumed that if the molecule passes through the permeable boundary during a time step of the simulation that there is a finite probability that it was absorbed. Such an event could occur in one of two ways. (i) The molecule began in the cytoplasm and the random displacement during a time step, Δt, moves it across the boundary (fig. 2). (ii) The molecule starts and ends inside the cytoplasm, but during that move it crossed the boundary then re-entered the cell. Such a move is plausible since Brownian motion is infinitely detailed, and therefore our step length is just an representation of the displacement, and should not be considered a precise trajectory.

The probability that a molecule crossed the boundary of the cell can be calculated given the initial and final perpendicular distances to the surface, l_i and l_f, respectively[11]. For case (i), if the molecule is outside of the cell at the end of the time step, it is obvious that the molecule crossed the boundary ($Prob(cross|l_f) = 1$). In case (ii),

$$Prob(cross|l_f) = exp\left(-\frac{2l_i l_f}{s^2}\right) \qquad (8)$$

While this method is exact only for planar surfaces, the curvature of the membrane is small compared to the average step size of the molecule, such that on pertinent length scales, the membrane is essentially flat.

If a molecule transiently interacts with the membrane (i.e. crosses the lattice boundary of the system), then there is a finite probability that it will bind to a site of the hexagonal lattice. While binding rates are known for MinD and MinE, these quantities are based on ensemble-averaged measurements and do not reflect important modulations based on single molecule interactions. The rates that Huang, *et al* use reflect long range recruitment interactions that span the entire grid spacing (50 nm). This is unrealistic and therefore not readily transferable to our representation. Instead we use a plausible energy function to describe short range protein-protein interactions. Such a function is meant to capture the qualitative strengths of associations, but does not accurately reproduce *in vivo* reaction rates.

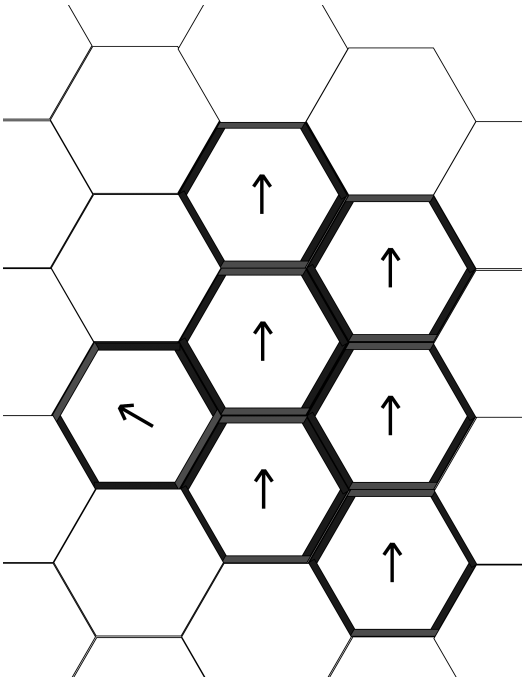

Figure 3: **Hexagonal lattice:** Schematic representation of MinD molecules bound to the hexagonal lattice. Each molecule has a specified orientation (arrow). Primary binding sites between molecules (gray edges of hexagonal unit), specify preferential orientation of binding. Secondary bindings sites (black edges), provide lateral stability to the filament.

In constructing an appropriate Hamiltonian the following assumptions are made that account for interactions onserved *in vivo* and *in vitro*: (i) MinD binds to the membrane in a self-enhancing directional fashion (zipper model) [4]; (ii) MinD is a polar molecule, such that MinE binds at one edge of the growing filament [4, 12]; (iii) Aggregates of MinD on the membrane surface increase binding probability of other MinD molecules in adjacent lattice positions and stability of the filament to disassociation or disassembly by MinE.

When a MinD molecule is found to cross the membrane boundary, a random orientation is selected and the change in energy ΔE is calculated. The probability that that molecule binds to the membrane in that position is given by,

$$Prob(bind|cross) = exp(-E_0 - E) \qquad (9)$$

where E_0 is an offset energy. E is the energy associated with nearest-neighbor interactions, where E is zero for a site with no neighbors and gets increasingly negative with increased neighbors in

the same orientation. Head-to-head alignment is preferentially biased over lateral associations in the same orientation. This is implemented by assigning two primary sites on each hexagonal subunit, and four secondary binding sites (fig. 3). Similarly, MinE binding to membrane-associated MinD:ATP relies on an energy function that penalizes binding away from the leading edge of a a growing MinD filament. MinE activated release of MinE and MinD from the membrane occurs at a constant rate.

MinD Linear Filament Formation

Suefuji, *et al.* demonstrated that purified MinD forms linear filaments in the presence of ATP, and that incubation with phospholipid vesicles enhances its polymerization [12]. Figure 4 shows exemplar results from a simulation meant to mimic Suefuji's *in vitro* experiment. Using a system with 4000 MinD molecules without any MinE in the system, resulted in the formation of linear filaments similar to those observed in [12], after 30 seconds of simulated 'real time' (See [12], figure 4). Filaments formed in random orientations, ranging in width from 5-10 molecules. As in the experiment, filaments formed quickly after 30 seconds and reached an equilibrium length and width that did not change noticeably when compared to simulations allowed to run for 2 minutes of real-time.

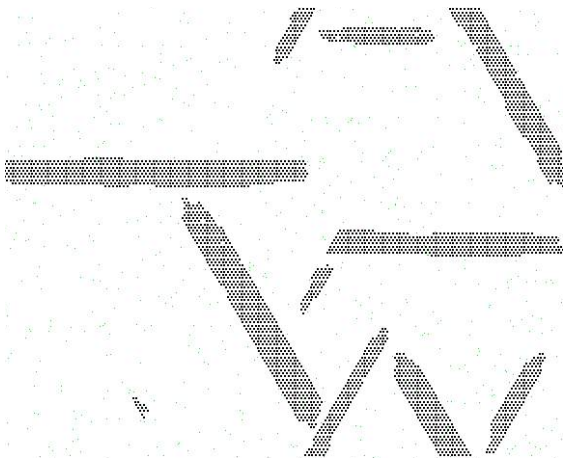

Figure 4: **MinD Linear Filament:** 4000 MinD molecules allowed to interact with the membrane in the presence of ATP for 30 seconds

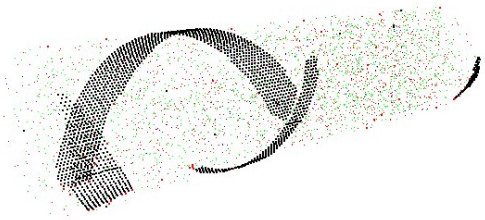

Figure 5: **Full Cell Simulation of Min protein dynamics:** 4000 MinD and 1400 MinE molecules after 40 seconds of simulated real-time, form helices that wrap around the inner membrane of the cell

Three Dimensional Full Cell Simulation of Min Pattern Formation

MinD aggregation originates in the polar zones of the cell [6]. It is possible that no additional constraints are needed to reproduce this observation, however as we were unable to search the large parameter space of the simulation, we posit the existence of nucleation sites at the poles in order to initiate filament formation. This assumption is not without biological motivation; although a specific accessory protein has not been identified that target MinD to a specific region of the cell in *E. coli*, DivIVA plays that role in *B. subtilis* [13]. Instead of including another species of molecule in our system, a small patch on each of the cell's membrane has an enhanced probability of binding MinD:ATP, as well as constraining the orientation of the MinD molecules that bind there.

This assumption in collaboration with selected binding affinities of MinD and MinE, results in 1-3 filaments originating primarily in the polar region of one end of the cell (fig. 5). While the helices generally spiral down the long axis of the cell, this appears to be an artifact of the simulation: (i) The pitch of the MinD helices is incorrect, as the hexagonal unit constrains the orientation of the MinD molecule to one of six possible directions. (ii) The filament can grow in the minus (-) direction (the end to which MinE cannot attach). As MinD polymerization reaches an equilibrium with transient unbinding and MinE driven disassociation,

MinD 'backfills' on the minus end and propagates unfettered.

The number and persistence of filaments were highly sensitive to the parameters selected. Small deviations resulted in many smaller filaments that did not form helices or large aggregates that blocked helical growth by volume exclusion. Several parameters sets were generated by making small perturbations around an initial guess. Each was tested and only a small range resulted in low numbers of propagating filaments. A substantial interdependency exists between the ratio of parameter values and the observed output of the simulation, therefore other subsets of parameters may yield similar results.

Simulations did not show proper oscillatory behavior as is observed *in vivo*. Since the primary mechanism of rapid MinD filament growth shifts to additions of MinD on the minus end as the plus end reaches an exchange equilibrium, MinE is not able to remove MinD from the front of the advancing filament. This breakdown of the oscillatory cycle is believed to be the primary cause of non-oscillatory behavior.

Discussion

This minimal model of the Min protein system in *E. coli* does not reproduce all of the pertinent *in vivo* observations from the experimental literature. This failure could be the result of (i) insufficient biological data necessary to create a realistic physical model, (ii) an incorrect set of model parameters, or (iii) a fallacious mathematical model of membrane binding and surface dynamics. Each represents an important vein of research that will be necessary in future revisions of this model. Most important among these is the necessity of a rigorous treatment of surface binding. A phenomenological energy function makes comparison to kinetic rate constants difficult. A hexagonal array, while providing a simple model-membrane, imposes unwanted constraints on our system. Allowing only the six discretized orientations defines the wrong helical pitch, an important physical characteristic that would help verify any model of the Min system. A continuous model of the membrane would remove such a constraint.

In this current model, MinD binds to the membrane in a fixed orientation. It is probable that these molecules are able to optimize locally due to rotational diffusion. This process is likely much faster than MinE binding and MinE mediated disassociation. Another possibility is that MinD can diffuse on the membrane surface, increasing the rate of polymerization. Future experimental results will place any such biological assumptions on steadier ground.

Acknowledgments

We thank Tom Carter and Melanie Mitchell for critical reading of the manuscript, and Adam Arkin for his assistance. J.L.A is supported by an NSF IGERT Fellowship. S.S.A is supported by a NSF post-doctoral fellowship in biological informatics.

References

[1] L.J.F Jones, R. Carballido López, and J. Errington. Control of cell shape in bacteria: Helical, actin-like filaments in *Bacillus subtilis*. *Cell*, 104:913–922, 2001.

[2] Z. Gitai and S. Shapiro. Bacterial cell division spirals into control. *Proc. Natl. Acad. Sci. USA*, 100(13):7423–7424, 2003.

[3] Y. Shih, T. Le, and L. Rothfield. Division site selection in *Escherichia coli* involves dynamic redistribution of Min proteins within coiled structures that extend between the two cell poles. *Proc. Natl. Acad. Sci. USA*, 100(13):7865–7870, 2003.

[4] T.H. Szeto, S.L. Rowland, C.L. Habrukowich, and G.F. King. The MinD membrane targeting sequence is a transplantable lipid-binding helix. *J Biol Chem*, 278(41):40050–40056, 2003.

[5] H. Meinhardt and P.A.J de Boer. Pattern formation in *Escherichia coli*: A model for the pole-to-pole oscillations of Min proteins and the localization of the division site. *Proc. Natl. Acad. Sci. USA*, 98(25):14202–14207, 2001.

[6] K.C. Huang, Y. Meir, and N.S. Wingreen. Dynamic structure in *Escherichia coli*: Spontaneous formation of MinE rings and MinD polar zones. *Proc. Natl. Acad. Sci. USA*, 100(22):12724–12728, 2003.

[7] M. Howard, A.D. Rutenberg, and S. de Vet. Dynamic compartmentalization of bacteria: accurate division in *E. coli*. *Phys Rev Lett*, 87(27):278102, 2001.

[8] Z. Hu, E.P. Gogol, and J. Lutkenhaus. Dynamic assembly of MinD on phospholipid vesicles regulated by ATP and MinE. *Proc. Natl. Acad. Sci. USA*, 99(10):6761–6766, 2002.

[9] K. Kruse. A dynamic model for determining the middle of *Escherichia coli*. *Biophys. J.*, 82(2):618–627, 2002.

[10] M. Howard and A.D. Rutenberg. Pattern formation inside bacteria: fluctuations due to the low copy number of proteins. *Phys Rev Lett*, 90(12):128102, 2003.

[11] S.S. Andrews and D. Bray. Stochastic simulation of chemical reactions with spatial resolution and single molecule detail. *Phys. Biol*, 1(3):137–151, 2004.

[12] K. Suefuji, R. Valluzzi, and D. RayChaudhuri. Dynamic assembly of MinD into filament bundles modulated by ATP, phospholipids, and MinE. *Proc. Natl. Acad. Sci. USA*, 99(26):16776–16781, 2002.

[13] A.L. Marston and J. Errington. Selecton of the midcell division site in Bacillus subtilis through MinD-dependent polar localization and activation of MinC. *Mol Microbiol*, 33(1):84–96, 1999.